# TECHNICAL PROGRESS REPORT

## A: COVER SHEET

Name of Submitting Organization: Nuonics, Inc.
Address of Submitting Organization: 1025 S. Semoran Blvd, Suite 1093, Winter Park, FL 32792
Tel/Fax: 407-379-0164

Name & Address of Sub-Contractor: University of Central Florida, 4000 Central Florida Blvd., CREOL Bldg, Orlando, FL 32816-2700

DOE Award No.: DE-FC26-03NT41923

Project Title: Ultra-High Temperature Sensors Based on Optical Property Modulation and Vibration-Tolerant Interferometry

Dated: Oct. 25, 2006.

Principal Author: Dr. Nabeel A. Riza (email: nriza@aol.com)

Period Covered by Report: April 1, 2006 – Sept. 30, 2006.
Type of Report: Semi-Annual Technical Progress Report

## B: ABSTRACT

The goals of the Year 2006 Continuation Phase 2 three months period (April 1 to Sept.30) of this project were to (a) conduct a probe elements industrial environment feasibility study and (b) fabricate embedded optical phase or microstructured SiC chips for individual gas species sensing. Specifically, SiC chips for temperature and pressure probe industrial applications were batch fabricated. Next, these chips were subject to a quality test for use in the probe sensor. A batch of the best chips for probe design were selected and subject to further tests that included sensor performance based on corrosive chemical exposure, power plant soot exposure, light polarization variations, and extreme temperature soaking. Experimental data were investigated in detail to analyze these mentioned industrial parameters relevant to a power plant. Probe design was provided to overcome mechanical vibrations. All these goals have been achieved and are described in detail in the report. The other main focus of the reported work is to modify the SiC chip by fabricating an embedded optical phase or microstructures within the chip to enable gas species sensing under high temperature and pressure. This has been done in the Kar UCF Lab. using a laser-based system whose design and operation is explained. Experimental data from the embedded optical phase-based chip for changing temperatures is provided and shown to be isolated from gas pressure and species. These design and experimentation results are summarized to give positive conclusions on the proposed high temperature high pressure gas species detection optical sensor technology.

# C: TABLE OF CONTENTS

## D: LIST OF GRAPHICAL MATERIALS

Figure 10: Interferometric signature from probe set-up with (a) the moderate soot deposited chip Clear face (b) Soot face.

Figure 11: Interferometric signature from probe set-up with (a) Moderately high soot deposited chip Clear face (b) Soot face.

Figure 12: IR Interferogram of the moderate soot deposited chip with wavelength tuning.

Figure 13: Interferogram of the high soot deposited chip with wavelength tuning.

Figure 14: Pictures of the soot side of the SiC soot deposited chips with (a) Very heavy soot layer (b) Quick heavy soot (Soot applied for 1 minute; some soot peeled off with handling), and (c) Very heavy soot for 1 minute with heat soak at 1150 $^{o}$C for 30 seconds.

Figure 15: Interferograms for the clear side of (a) Very heavy soot (b) Quick heavy soot and (c) Very heavy soot with heat soak at 1150 $^{o}$C for 30 seconds.

Figure 16: IR interferograms of the chip placed in the acid for (i) 1 hour and (ii) 24 hours.

Figure 17: IR interferograms of the chip placed at 1100 $^{o}$C for (i) 30 minutes and (ii) 2 hours.

Fig.18 Proposed compact fiber-connected SiC frontend sensor designs for (a) temperature and (b) pressure sensing. E: Electrical wire for optional Motion Control Stage (MCS) packaged with a SMF within a protection cable. S: Spherical Lens; C: SiC Chip. SMF: Single Mode Fiber.

Fig.19. Designed laboratory MCS head fitted with fiber lens.

Fig.20: Reflected power from non-microstrured SiC chip as a function of temperature up to 350°C at normal incidence angle of the laser beam.

Fig.21: Experimental setup for laser metallization of the SiC chip (Kar Lab).

Figure 22: Sensor design with microstructured and non-microstructured sections.

Figure 23. Reflected power from microstructured SiC chip section as a function of temperature up to 500°C at normal incidence angle of the laser beam.

Figure 24. Reflected power from microstructured SiC chip section as a function of temperature up to 700°C at normal incidence angle of the laser beam.

Figure 25. Geometrical sketch and photos of laser-fabricated SiC chip: (a) Schematic drawing of a SiC chip showing the laser-embedded sensing microstructure, (b) View for top surface B showing the top view of the microstructure, (c) View for bottom surface C at which the growth of the chip microstructure nucleated for this sample, (d) View for side surface D showing the thickness of the embedded chip and (e) View for side surface E showing the thickness of the embedded SiC chip.

Figure 26. Project activities for SiC chip development, sensor fabrication and optical response studies.

## E: INTRODUCTION

The purpose of this project is to develop a science base to fabricate sensors for ultra high temperature fossil fuel applications. The sensors proposed are based on the principle of the Optical Path Length (OPL) variation in a medium owing to the dependence of the optical property (e.g., refractive index) of a high temperature material, such as silicon carbide (SiC), on the temperature, pressure, or species concentration. These three thermodynamic variables can be measured by a single sensor if we understand how they individually change the refractive index of the sensor material. Since these changes can be very small, a high accuracy optical signal processing scheme is proposed for working in unison with the remote SiC sensor frontend. Specifically, a vibration-tolerant interferometric technique capable of measuring the changes in OPL with sub-nanoscale accuracy and at a high speed is investigated in this project. The proposed novel sensor technique will thus enable us to measure the desired variables remotely, accurately and rapidly.

Remote interrogation of the sensor by using a laser beam will eliminate the complications associated with electrical signal-based sensors in high temperature applications. The complications in such conventional sensors include (i) melting of the solder joint between the sensor device and the bonding wire, (ii) requirement of high temperature insulation for the electrical wires connecting the device to the electrical signal processing unit, and (iii) inconvenience in mounting or embedding the device in rotating components such as the turbine blades. A high speed optical interferometer can respond to the changes in the thermodynamic variables rapidly at microsecond speeds allowing real-time control of the combustion process.

Since a passive sensor frontend chip is proposed, any optically transparent high temperature material, such as a single crystal silicon carbide, diamond or sapphire, can be used as the sensor

chip material. Such a passive sensor chip can be custom fabricated for specific gas species detection and produced at low cost in a small (sub-millimeter) size and can be readily embedded in a small hole at the surface of any structure by using the thermal expansion/contraction stress-based fitting method. The structure could be a stationary or rotating component containing the sensor at a convenient location providing remote accessibility to the probe laser beam for interferometry.

Note that the leading fiber-optic sensors such as using fiber Fabry-Perot interference or in-fiber Bragg Gratings with wavelength-based processing require costly environmental protection of the light delivery and light return fiber [1-3]. This is because the fiber intrinsically contains both the sensing zone that must react to the changing environmental conditions (e.g., temperature) and the light delivery fiber that should stay protected and essentially unaffected from changing environmental effects (e.g., changing stresses in the long lengths of the delivery fiber could cause unexpectedly high bending losses leading to loss of detection signal). It is well known that standard low loss single mode optical fibers (SMFs) are made of glass, with transition temperatures around 475 °C, leading to unwanted softening of glass at higher temperatures, such as needed in DOE applications. Thus, there exists a dilemma for the sensor design engineer using the mentioned fiber-optic sensors. In our proposed sensor, this dilemma is removed as a free-space laser beam reads sensing parameters off the SiC sensor chip, thus producing no physical contact between the harsh environment and the light delivery and processing optics. In effect, one can imagine many low cost SiC optical chips distributed in the desired sensing zone where a scanning free-space laser beam rapidly engages these sensor frontend chips to produce signals for later data processing and environmental parameter recovery. In effect, a truly non-invasive distributed optical sensor is realized.

## F: EXECUTIVE SUMMARY

Accomplishments during the three months of this project have been achieved on two fronts, namely; (a) Sensor probe elements industrial feasibility assessment study and (b) Embedded optical phase or microstructured SiC chip fabrication and testing for high temperature gas species sensing application.

The first primary objective was achieved by engaging with a major power generation systems design house turbine test facility that today utilizes extreme temperature and high pressure probes to make temperature and pressure measurements within a power plant. Specifically, industrial power plant soot was generated directly on the SiC sensor chips to test fundamental sensor operational survivability under power plant conditions of various soot levels. The chips were then also tested for handling high temperature heat soak and long exposure to corrosive acid chemicals. The chip sensing behavior was studied under varying light polarization conditions. Probe designs were proposed for handling mechanical vibrations and initial hardware was assembled.

The second primary objective was achieved by designing and building a laser-based embedded optical phase SiC chip generation system. The system was used to produce a chip with one side containing the desired embedded optical phase or microstructures suitable for making a gas species discrimination chip. Different optical responses for the two sections, i.e., non-microstructured and microstructured of the chip where used to isolate chip response to temperature versus gas species and pressure. This concept is intended for discriminating between various gas species, given custom embedded optical phase microstructured chips for specific gas species.

## G: EXPERIMENTAL RESULTS

### G.1 Sensor Probe Elements Industrial Feasibility Assessment Study:

#### G.1.1 Fabricated SiC Chips Sensing Quality and Polarization Robustness Tests:

Each fabricated SiC chip has a characteristic interferometric signature resulting from the interference of the light reflecting from the chip. Figure 1 shows the experimental setup used to get the interferometric signatures of each of the thirty-seven 1 cm x 1cm square 400 micron thick fabricated 6H single crystal SiC chips. These signature then tell the optical quality of the chips and their appropriateness for sensor design.

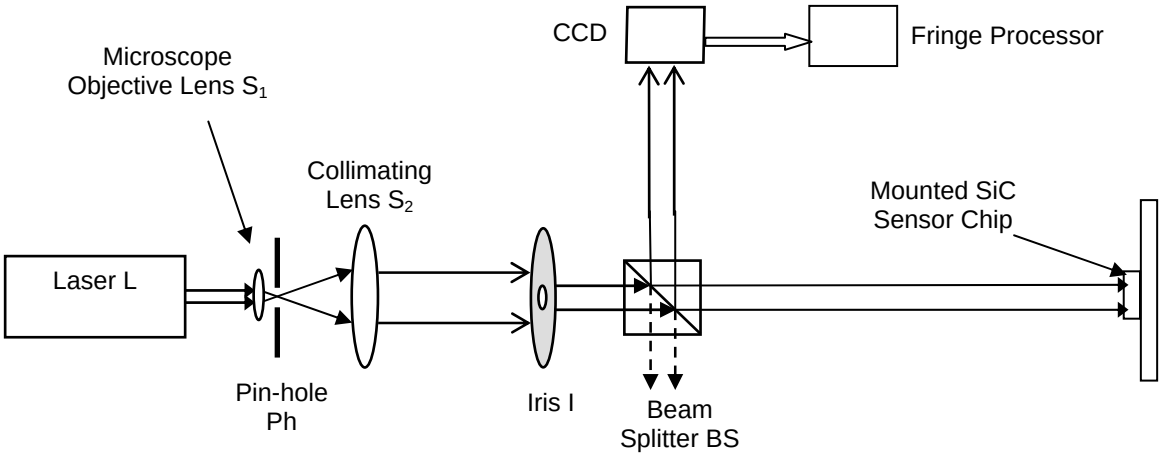


Figure 1: Experimental setup to obtain the interferometric signature of SiC chip.

He-Ne laser ($\lambda = 633$ nm) is used in this experiment while the incident beam size on the SiC chip is 5 mm in diameter. The interferometric signatures obtained for the SiC chips are shown in Figure 2.

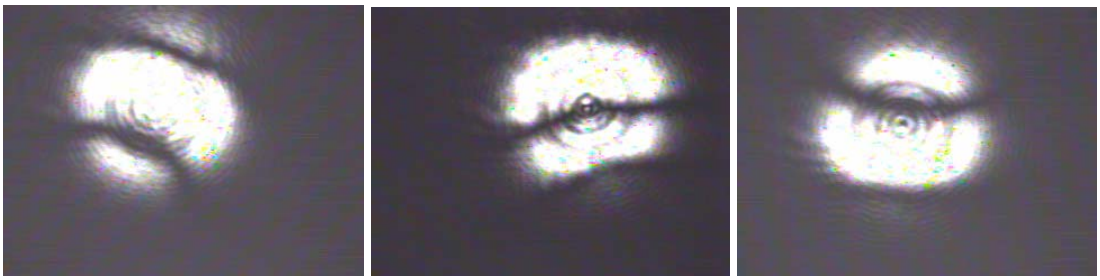

(i) (ii) (iii)

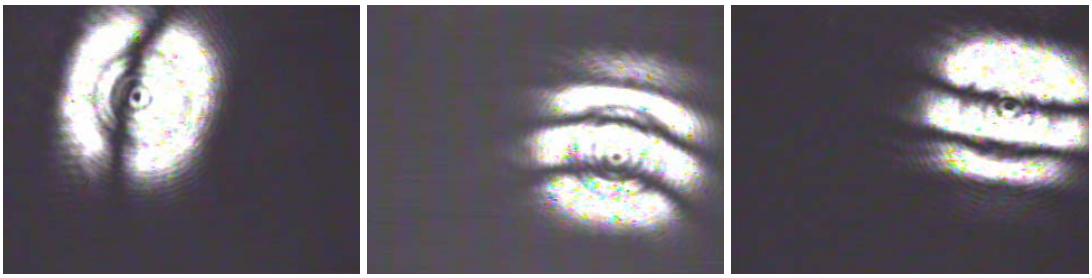

(iv) (v) (vi)

(vii) (viii) (ix)

(x) (xi) (xii)

Figure 2 (i) – (xxxvii): Interferometric signatures (@ 633 nm)of the fabricated SiC chips.

(xiii) (xiv) (xv)

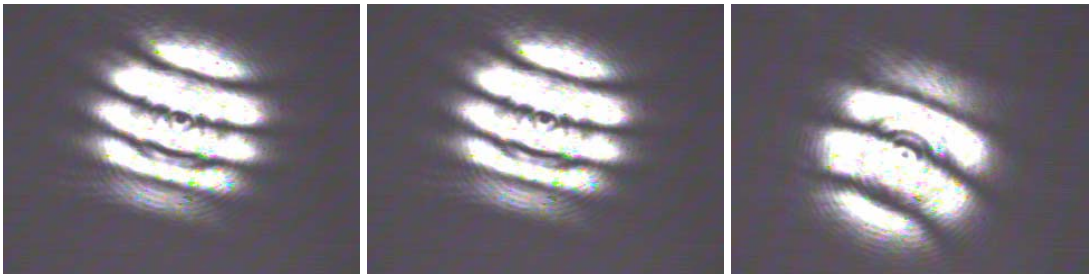

(xvi) (xvii) (xviii)

(xix) (xx) (xxi)

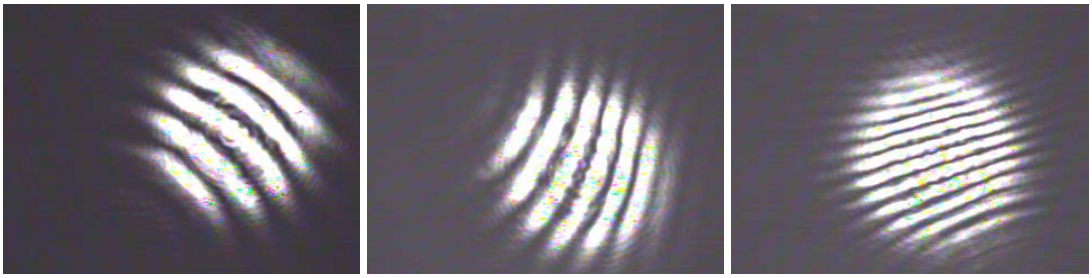

(xxii) (xxiii) (xxiv)

Fig.2 (Continued).

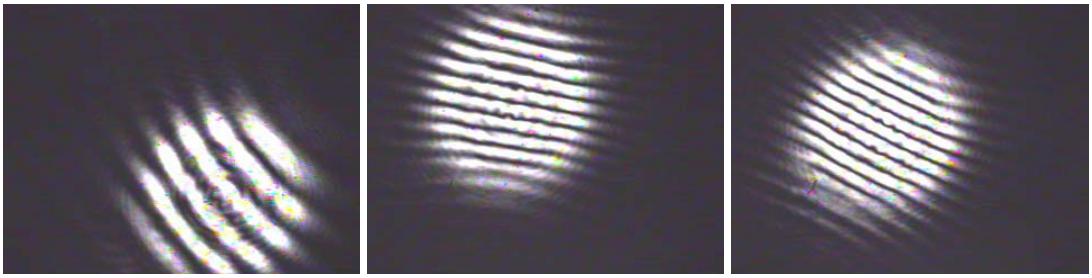

(xxv) (xxvi) (xxvii)

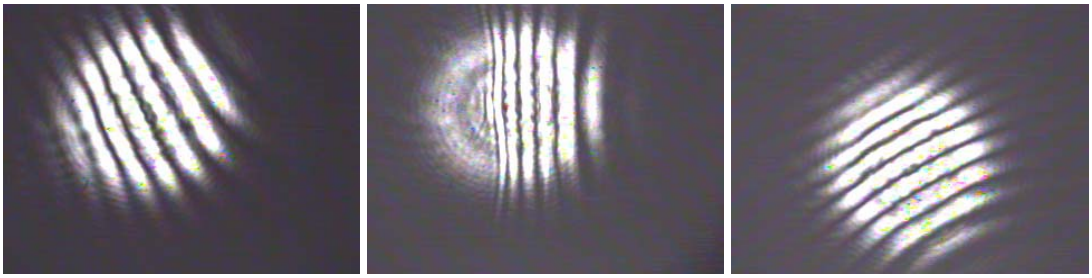

(xxviii) (xxix) (xxx)

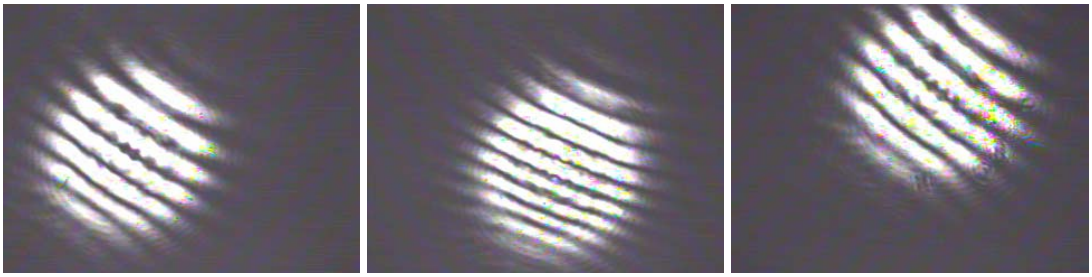

(xxxi) (xxxii) (xxxiii)

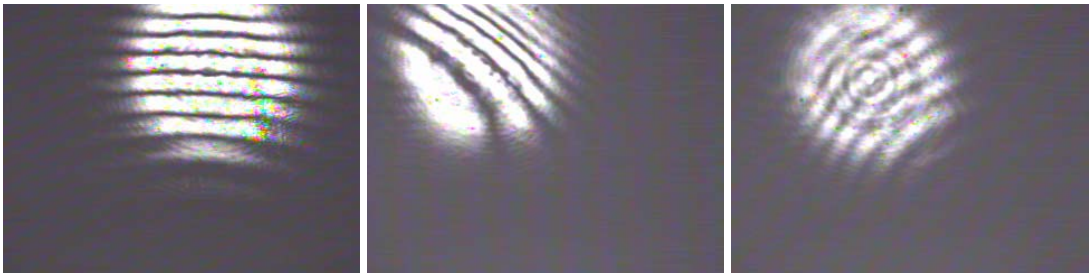

(xxxiv) (xxxv) (xxxvi)

Fig.2 (Continued).

(xxxvii)

Fig.2 (Continued).

Based on the number of fringes observed in the 5 mm diameter spot, chips number (i)-(iv) in Figure 2 were classified as good while chips number (v)-(xix) were classified as as moderately good and chips number (xx)-(xxxvii) were deemed non-optimal for use in the probe.

The good chips are chosen for probe assembly and checked for polarization independence (an important attribute when designing the probe) using a polarizer and Liquid Crystal (LC cell) as shown in Figure 3.

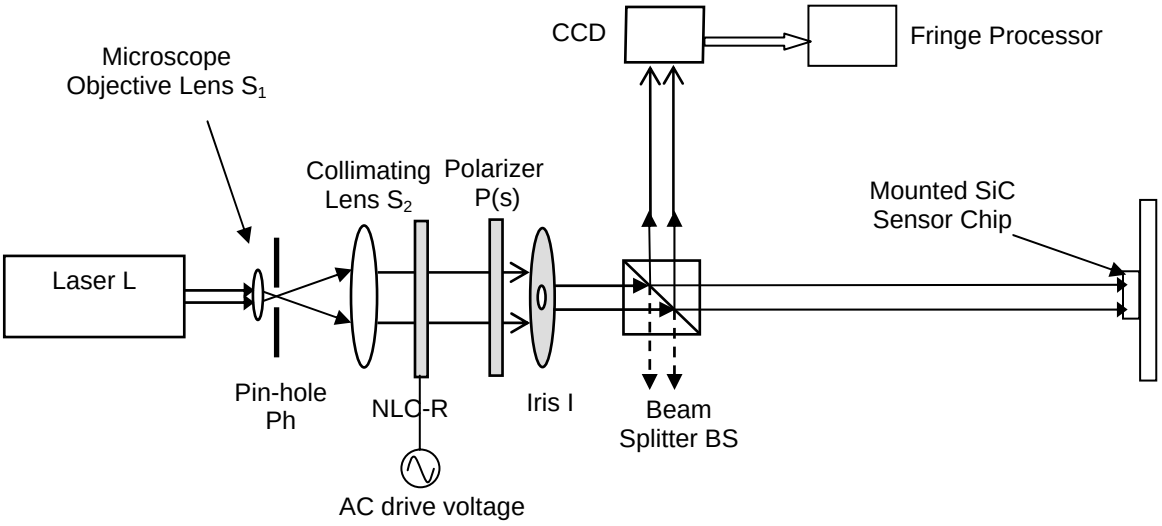


Figure 3: Experimental setup for checking polarization dependence of the SiC chip

Figure 4(i): Observed interferograms with general change in probe light polarization.

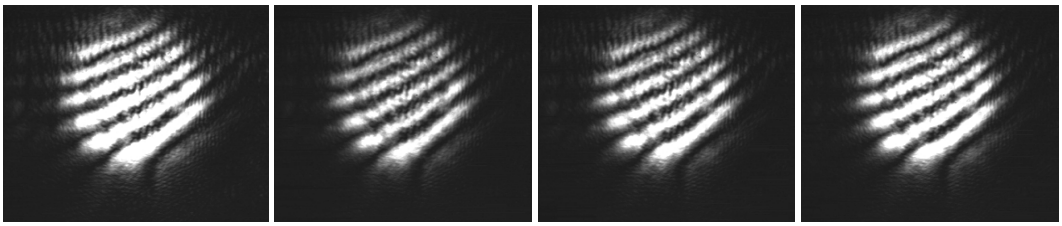

(a) (b) (c) (d)

Fig.4 (ii) Recorded interferograms off the SiC chip for incident light linear polarization angles of (a) $0^0$ (b) $45^0$ (c) $90^0$ and (d) $135^0$. Observed optical beam diameter is 5 mm. Wavelength used is 633 nm.

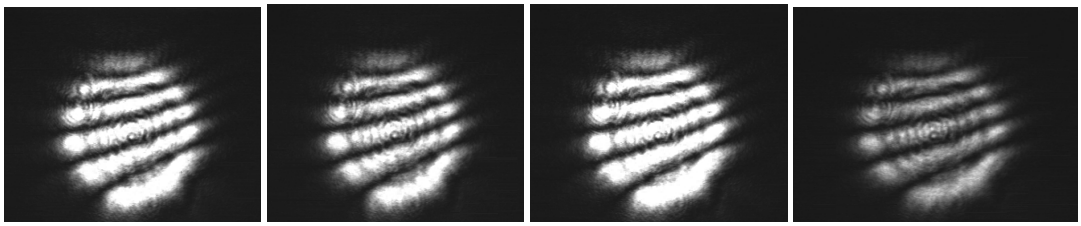

(a) (b) (c) (d)

Fig.4(iii) Recorded interferograms off the SiC chip for incident light elliptical polarization state of (a) Eccentricity = 0.69, Tilt = $45^0$ (b) Eccentricity = 0.99, Tilt = $29.4^0$ (c) Eccentricity = 0.98, Tilt = $9.4^0$ (d) Eccentricity = 0.83, Tilt = $7.6^0$

These interferogram results are shown in Figure 4(i,ii,iii) and show that interference fringes do not move with change in polarization, indicating the robustness of sensor performance using the proposed chips.

**G.1.2 Probe Design Bench Tests for Polarization Robustness:**

Figure 5 shows the Infrared (IR) band probe design bench test set-up for the chosen optimal SiC chips selected from the general batch of fabricated SiC chips. Here, the tunable laser has a wavelength tuning range of 1520-1600 nm. The fiber Graded Index (GRIN) lens forms its $1/e^2$ minimum beam waist at a distance of 25 cm from the lens. The under test SiC chips are placed at a distance of 44.5 cm from the lens which is the expected minimum length of the probe.

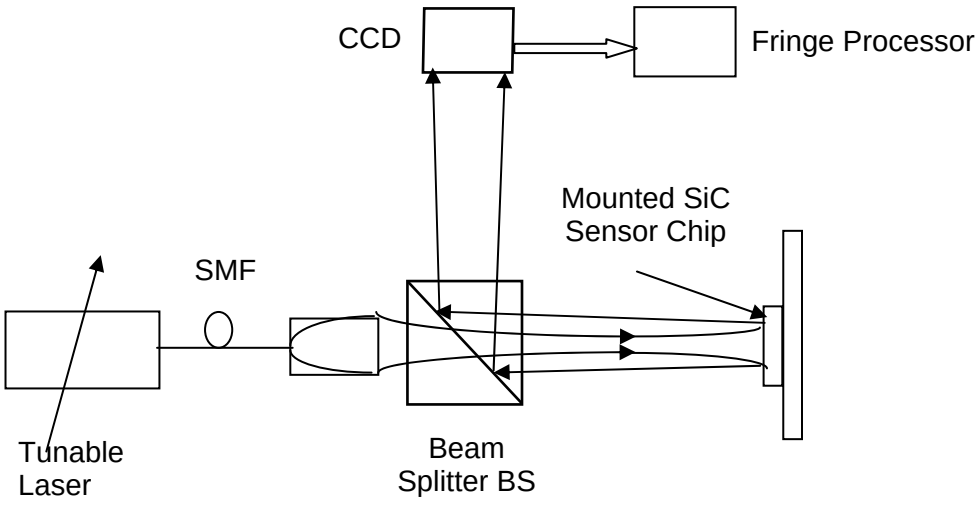


Figure 5: Infrared (IR) band probe design bench test set-up.

Figure 6 shows the beam imaged on the CCD when a plane mirror is placed in place of the SiC chip in the setup of Figure 5. The size of the beam as measured on the CCD is found to be 3.6

mm. Since the beam keeps on diverging, this implies that the size of the beam when it strikes the mirror is more than 3.6 mm.

Figure 6: Image of the IR beam in the probe when reflected by a plane mirror.

Chip (xxi) is now placed in the probe setup and the interferogram is observed on the CCD. As predicted by interference theory, the spatial frequency decreases at a higher wavelength and hence fewer fringes are observed in IR as compared to the visible (see Figure 7 (a) and 7 (b)). To verify that the fringes observed are indeed caused by interference, the wavelength is tuned and the fringes are observed to move (Figure 7 (c) and (d)).

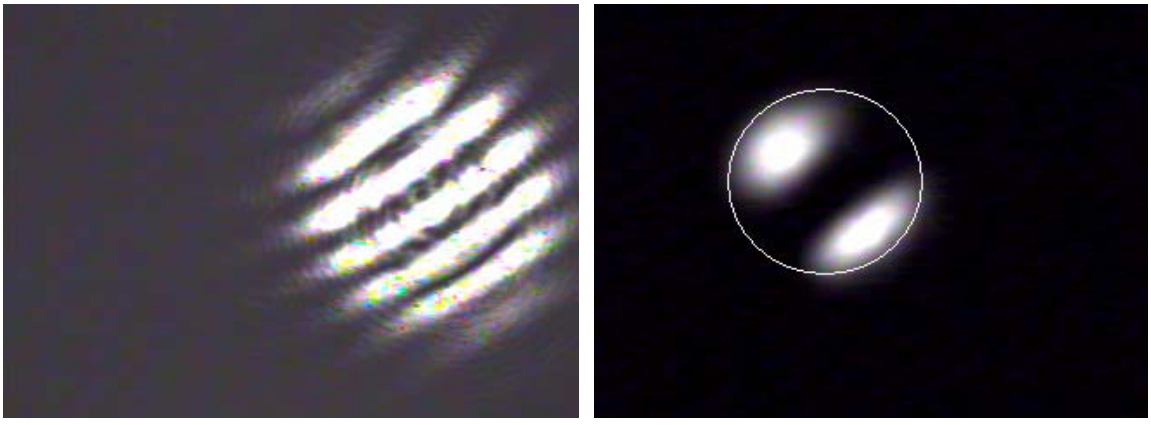

(a) (b)

Figure 7: Chip (xxi) interferograms from probe for (a) visible 633 nm (b) IR 1560.66 nm.

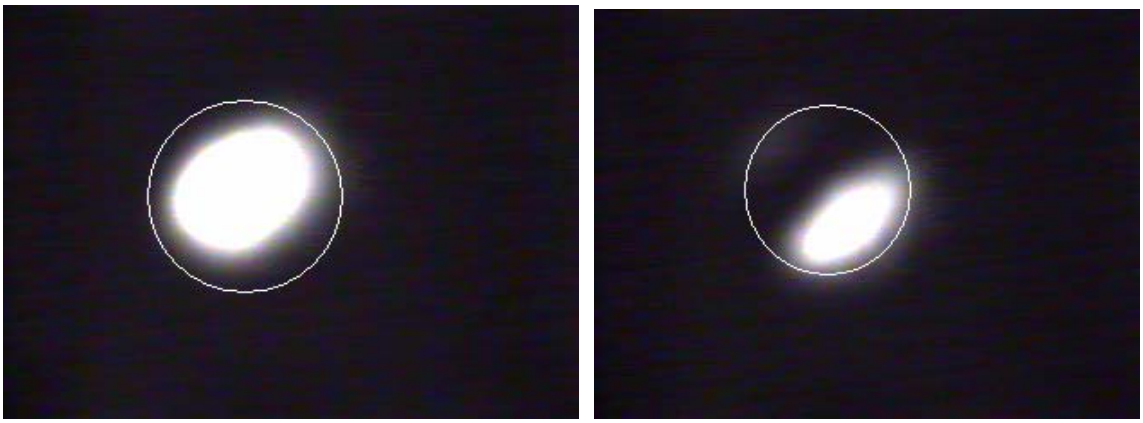

(c) (d)

Figure 7: Chip (xxi) interferograms from probe for (c) IR 1561.02 nm (d) IR 1561.31 nm.

The polarization insensitivity of this chip is also checked in IR using a fiber-optic polarization controller. The fringes are again observed not to move with change in polarization (see Figure 8).

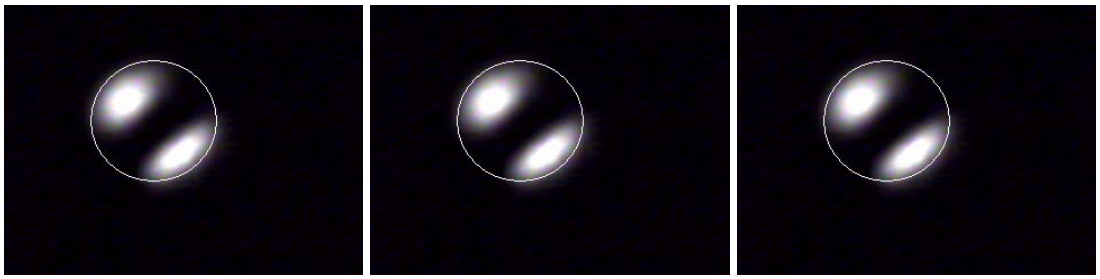

Figure 8: Observed IR interferograms from probe with changes in input polarization.

The modulation depth of the interferograms is calculated as:

$$M.D = \frac{I_{\max} - I_{\min}}{I_{\max} + I_{\min}}$$

The theoretical value of the modulation depth as given by using the Fresnel reflection coefficients for SiC in the IR band is found to be 0.977. The experimental value found by image processing the IR detector performance limited interferograms is 0.785.

### G.1.3 Probe Design Bench Tests for Industrial Soot Robustness:

In coal-driven power plants, soot is generated as a by-product. Thus, it is expected that when the temperature probe is inserted into the gas turbine, soot will be deposited on one side of the SiC sensor chip. At our industrial power plant partner test facility, first SiC chips numbers (xxxi) and (xxxiii) have soot deposited on one side using an oxy-acetylene flame as a gas mixture can be safely varied to control the level of soot in the flame to generate power plant soot conditions. Chip (xxxi) is deposited with moderate soot while chip (xxxiii) is deposited with moderately high soot. Figure 9 shows the microscopic photographs of the soot face of the two chips and the clear face of the moderately high soot chip. The figures show that when looking from the clear side of the chip, the soot is not visible in the microscopic view.

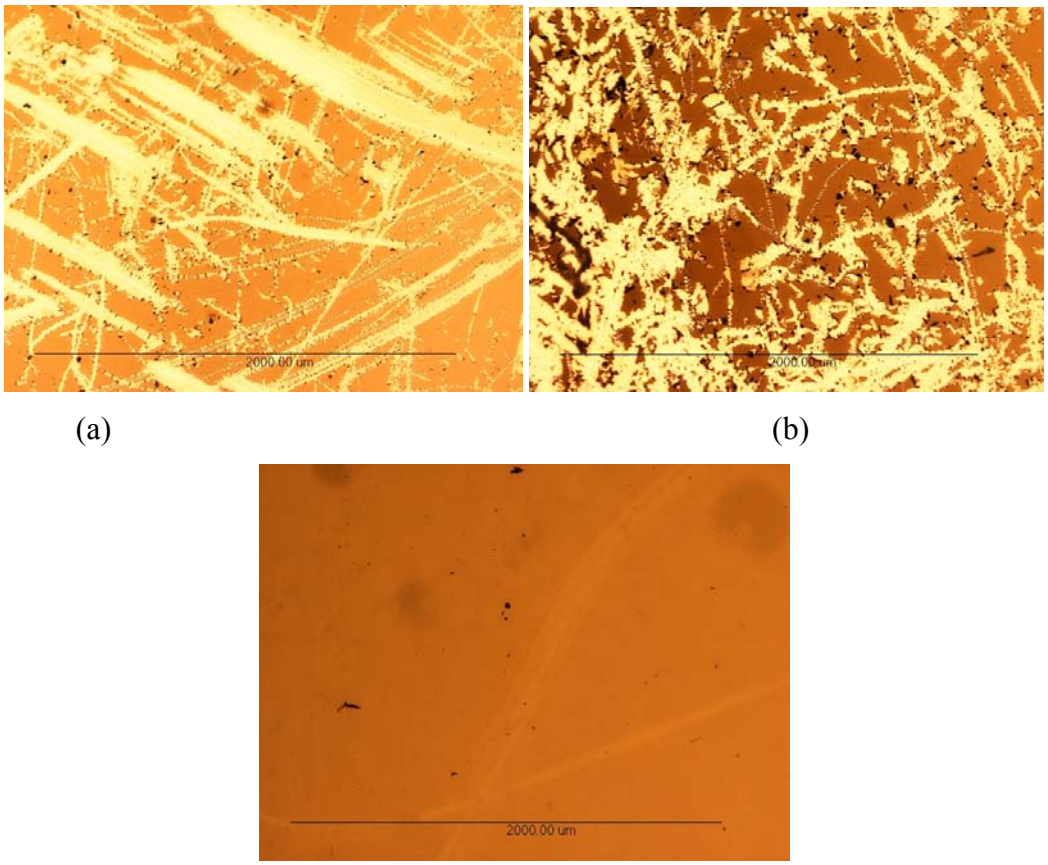


(a) (b)

(c)

Figure 9: Microscopic photographs of SiC chip faces with (a) moderate soot and (b) moderately high soot levels and (c) a clear chip with no soot.

These chips are then put under test again in the setup of Figure 1. The results (Figure 10 and Figure 11) show that when the light is incident on the clear face of the chip, as would be the case in the proposed probe design, there is no change in the interferometric signature of the chip but when the light is incident on the soot face, the interferogram is covered with a random phase mask thus destroying it, an effect especially visible with the high soot chip.

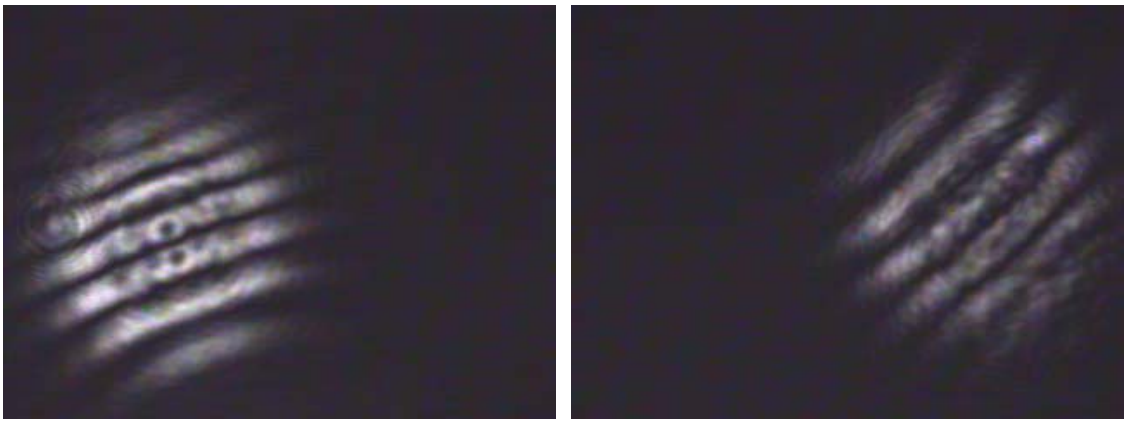

(a) (b)

Figure 10: Interferometric signature from probe set-up with (a) the moderate soot deposited chip Clear face (b) Soot face.

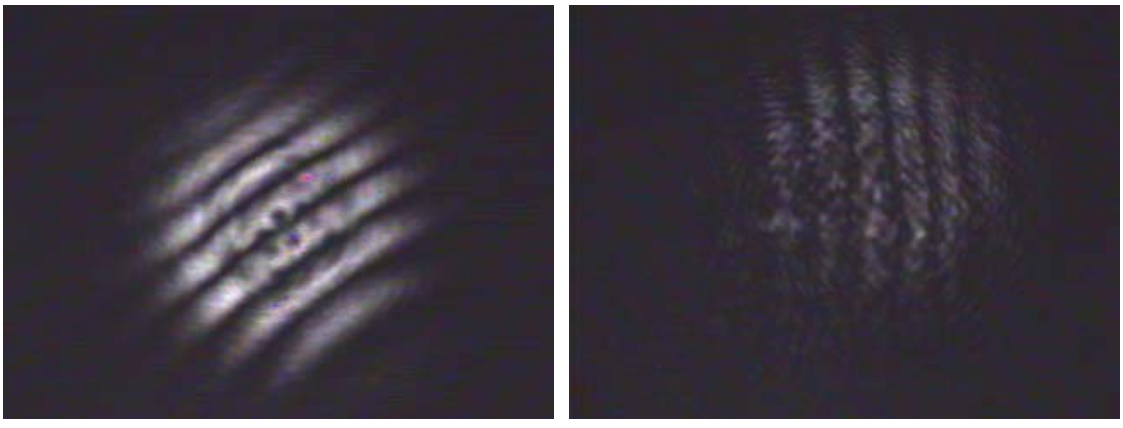

(a) (b)

Figure 11: Interferometric signature from probe set-up with (a) Moderately high soot deposited chip Clear face (b) Soot face.

These chips are then taken to the IR probe setup of Figure 5 and the interferograms are again observed for the clear side. The results are shown in Figure 12 and Figure 13. Again, it is observed that for the light incident on the clear side, there is no change in the interferogram and its behavior with wavelength tuning.

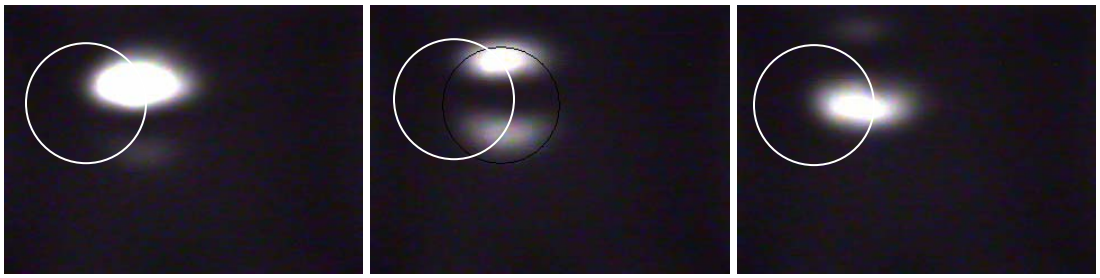

Figure 12: IR Interferogram of the moderate soot deposited chip with wavelength tuning.

Figure 13: Interferogram of the high soot deposited chip with wavelength tuning.

Next, SiC Chips (xxiii) and (xxxi) are now deposited with very heavy soot and quick heavy soot, respectively. Chip (xxxiii) is deposited with very heavy soot for around 1 minute and then heat soaked with a high temperature torch at 1150 $^{o}$C for 30 seconds. The laboratory pictures of the three sooted chips are shown in Figure 14. In these cases, the soot is so dense that no features are visible using a microscope as light is completely absorbed.

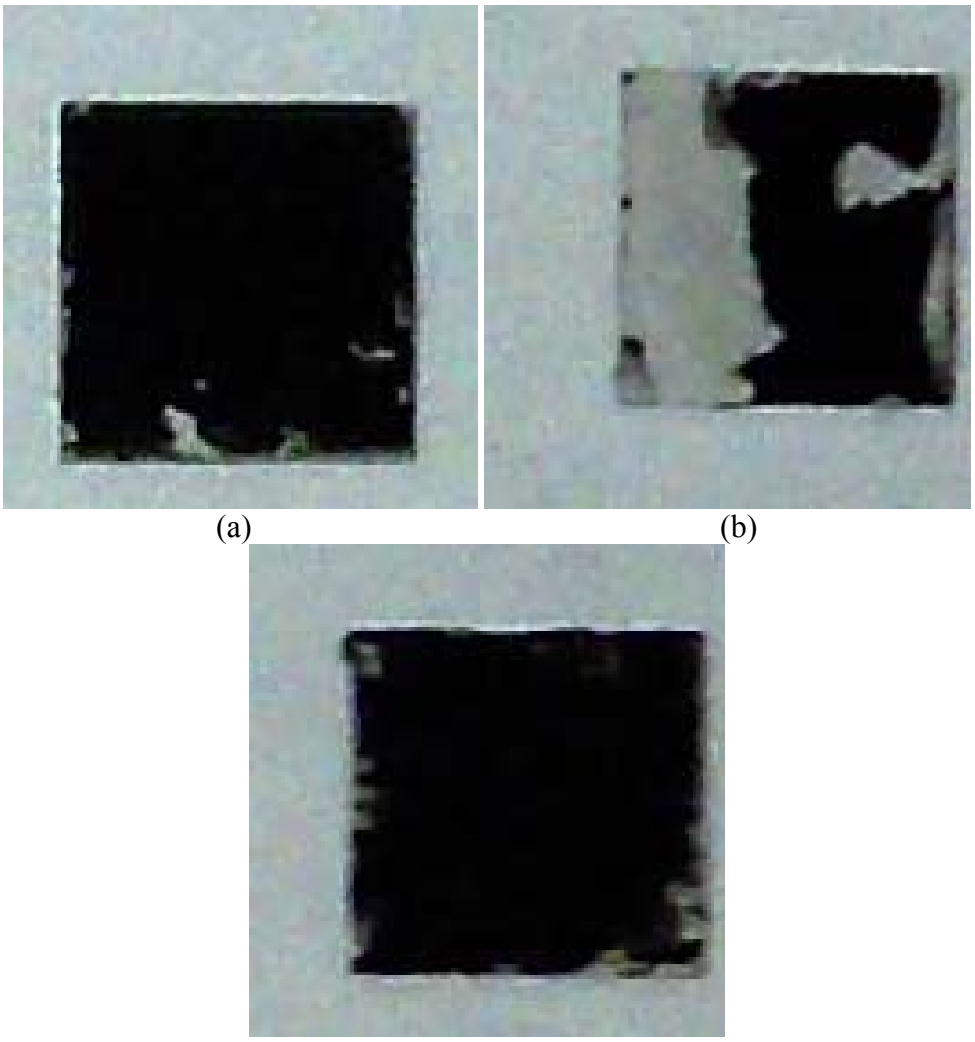

(a) (b)

(c)

Figure 14: Pictures of the soot side of the SiC soot deposited chips with (a) Very heavy soot layer (b) Quick heavy soot (Soot applied for 1 minute; some soot peeled off with handling), and (c) Very heavy soot for 1 minute with heat soak at 1150 $^{o}$C for 30 seconds.

These chips are put under test again with their clear side facing the light beam in the IR probe setup of Figure 5. The interferograms obtained are shown in Figure 15. The interferograms show that there is still no distortion when light is incident on the clear face of the chip in the probe set-up.

(a) (b) (c)

Figure 15: Interferograms for the clear side of (a) Very heavy soot (b) Quick heavy soot and (c) Very heavy soot with heat soak at 1150 $^{o}$C for 30 seconds.

**G.1.4 Probe Design Bench Tests for Industrial Chemical & Sustained Temperature Robustness of SiC Chips:**

The Single crystal 6H-SiC chips are next tested with harsh chemicals and sustained extreme temperatures. To check whether corrosive chemicals would have an effect on the SiC chip, chip (xx) is placed in concentrated Sulphuric Acid for a period of up to 24 hours. The chip is then put under test in the setup of Figure 5. Figure 16 (i) and (ii) show the interferograms obtained after 1 hour and 24 hours in the acid respectively. The figure clearly shows that there is no change in the interferograms after being placed in the acid.

(i) (ii)

Figure 16: IR interferograms of the chip placed in the acid for (i) 1 hour and (ii) 24 hours.

Chip (xxi) is placed in an oven at a temperature of 1100 $^{o}$C sustained for a period up to 2 hours.

The chip is then cooled and put under test again in the set-up of Figure 5. Figure 17 (i) and (ii) show the interferograms obtained after 30 minutes and 2 hours in the oven, respectively. As demonstrated by Figure 17, no change is observed in the interferograms in either case.

(i) (ii)

Figure 17: IR interferograms of the chip placed at 1100 $^{o}$C for (i) 30 minutes and (ii) 2 hours.

### G.1.5 Vibration Robust Probe Designs

As shown in our studies, single crystal 6H-SiC is a highly desirable front-end sensor material as its melting temperature is around 2500 $^{0}$ C. Moreover, apart from its resistance to chemical attack and excellent optical properties, thick (e.g., 400 μm) single crystal 6H-SiC also has powerful mechanical properties via its elastic, shear, and bulk modulus values and Poisson ratio. Therefore, the SiC chip forms a robust extreme environment front-end sensor for laser beam-based wireless access. Nevertheless, fiber-optics can play an important role in the proposed hybrid sensors by providing a wired light delivery mechanism to the wireless port position in the sensor system. Well protected custom Single Mode Fibers (SMFs) made of silica can operate near temperatures reaching 1000 °C , thus forming an excellent wired non-line of sight delivery mechanism to a location near the extreme environment where temperatures are still reasonable compared to the extreme environment temperature (e.g., 1500 °C in a combustion chamber).

Fig.18 shows some example Nuonics designs under study showing how SMFs can be combined with the proposed SiC chip-based sensing principles to realize compact versions of the remoted hybrid sensors. In essence, the distance between the SiC chip and the launch SMF point

is small, forming an all-in-one compact fiber remoted sensing head, much like traditional SMF sensors.

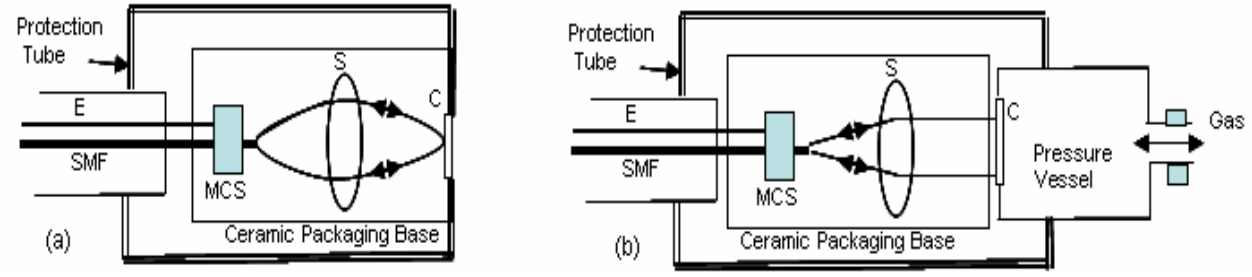


Fig.18 Proposed compact fiber-connected SiC frontend sensor designs for (a) temperature and (b) pressure sensing. E: Electrical wire for optional Motion Control Stage (MCS) packaged with a SMF within a protection cable. S: Spherical Lens; C: SiC Chip. SMF: Single Mode Fiber.

Fig.18(a) shows a temperature sensor design that is based on localized or point targeting of the SiC chip to measure temperature dependent optical path length change (OPL). By making the light read zone on the chip small compared to the chip size, one can essentially remove the effects of pressure on the chip localized OPL. Such targeting is achieved using a point-to-point imaging lens formation between the SMF-free-space interface and the SiC chip C. Because the proposed chip thickness is small (e.g., 400 μm) versus the imaging lens focal length (e.g., 3 cm) deployed, the chip front and back faces retro-reflect the sensing light back to the SMF for sensor signal processing. Each SMF can have an optional electronically controlled tilt control stage to keep the SMF aligned with the SiC chip. The entire assembly can be mounted in an appropriate ceramic package. To enable a pressure sensor, a collimating optical beam architecture shown in Fig.18(b) is used where the entire chip C is illuminated. As relative pressure between the chip

sides builds, the chip deforms and acts like a convex mirror, reducing the optical coupling between the SMF and the chip. Hence, a pressure change causes wavefront optical beam spoiling. As SMFs are very sensitive to wavefront quality, one sees a different coupling efficiency. Thus by monitoring the SMF coupling efficiency, pressure can be estimated assuming the chip packaging is designed such that temperature variations cause minimal chip deformation effects. In case temperature effects should not be ignored, both temperature plus pressure must be measured to generate a calibration table for optical coupling efficiency.

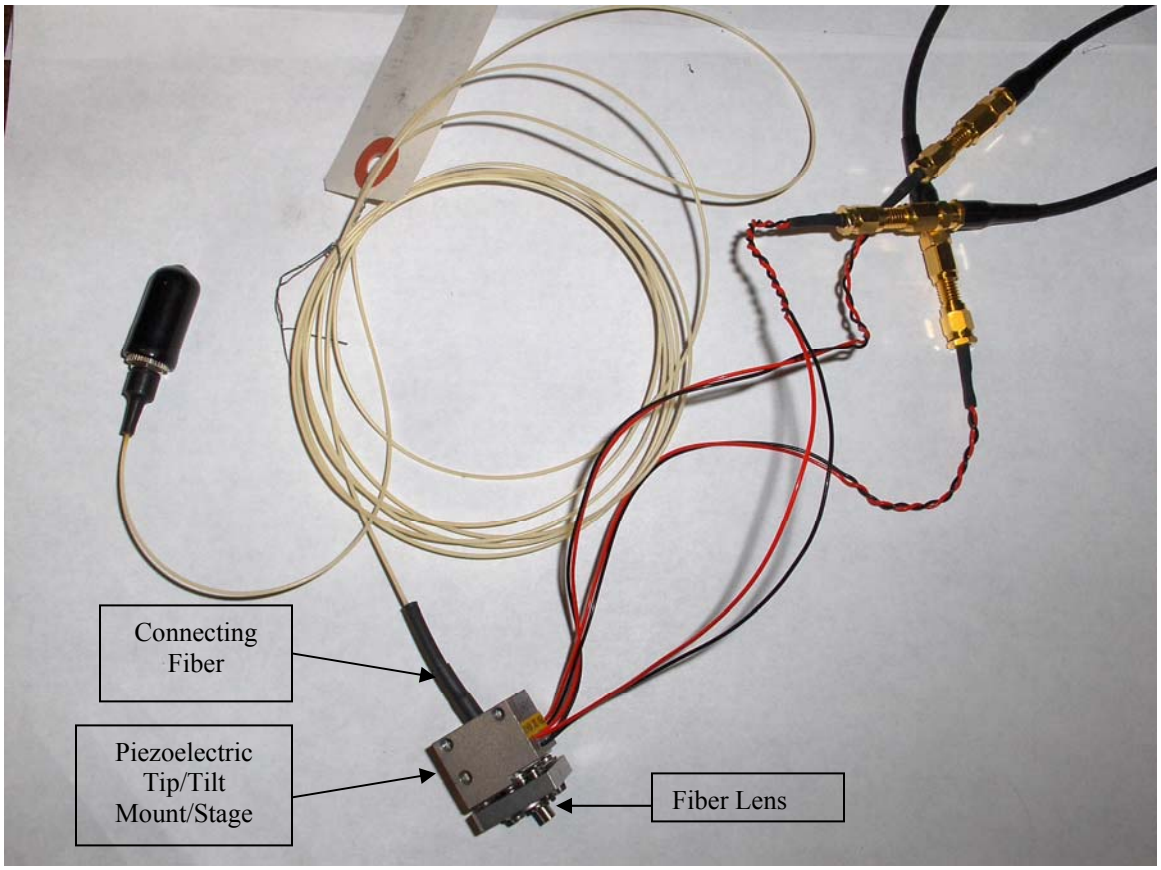


Fig.19. Designed laboratory MCS head fitted with fiber lens.

**G.2 Embedded Optical Phase/Microstructured SiC Chip fabrication and testing for high temperature gas species sensing:**

The optical properties (e. g., refraction index and reflectivity) of SiC depend on different thermodynamic states of combustion gases such as temperature, pressure and gas species. The changes in optical properties can be monitored with a laser beam and the characteristics (e.g., reflected power and polarization) of the reflected laser beam (optical signal) can be analyzed to determine the temperature, pressure and gas species. It should be noted that the optical signal contains data involving all of these three thermodynamic variables and, therefore, the signal needs to be analyzed in a systematic way to decouple these variables as outlined below:

1. Fabricate a SiC chip whose response depends on temperature only. This is done by fabricating an embedded optical absorber (laser-microstrured layer) in the SiC chip.
2. Obtain optical signals from the non-microstrured section of the SiC chip by varying the temperature of the chip and applying pressure to the chip using the same gas.
3. Obtain optical signals from the non-microstrured section of the chip by varying the temperature of the chip and applying pressure to the chip using different gases. We will have to sensitize the chip surface by laser doping in order to enhance the optical response of the chip for different combustion gases.

Steps 1 and 2 will allow decoupling of the temperature and pressure data, while steps 2 and 3 will allow decoupling of the gas species information from the temperature and pressure data. Representative data are presented in this report pertaining to steps 1 and 2. The interference pattern obtained in step 2 needs to be analyzed to decouple the temperature and pressure data.

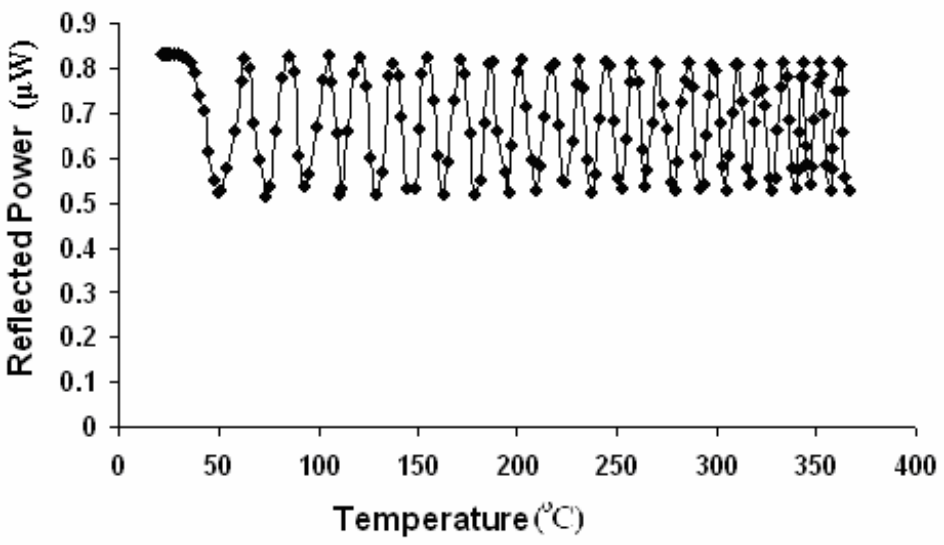


Fig.20: Reflected power from non-microstrured SiC chip as a function of temperature up to 350°C at normal incidence angle of the laser beam.

A He-Ne laser beam of wavelength 632.8 nm was directed to a SiC chip using an experimental setup. The temperature of the chip was varied from 20 °C to 500°C and 20°C to 700°C in two experiments and 50 psi nitrogen gas pressure was applied to the chip surface. The reflected power exhibited an oscillatory pattern (see Fig.20), i.e., the optical response was not monotonically increasing or decreasing as a function of temperature and gas pressure. Therefore such data cannot be used directly to measure temperature and pressure using SiC as a chip in practical applications. To obtain a better optical response that can be used directly for temperature and pressure measurements, the microstructure inside SiC chip was modified by irradiating the wafer with a high intensity Nd:YAG pulsed laser beam in the presence of methane gas at 30 psi pressure. This laser-embedded microstructuring process in which localized heating by the high intensity laser beam disorders the crystalline structure of SiC and produces carbon-rich phases which usually exhibit metal-like properties.

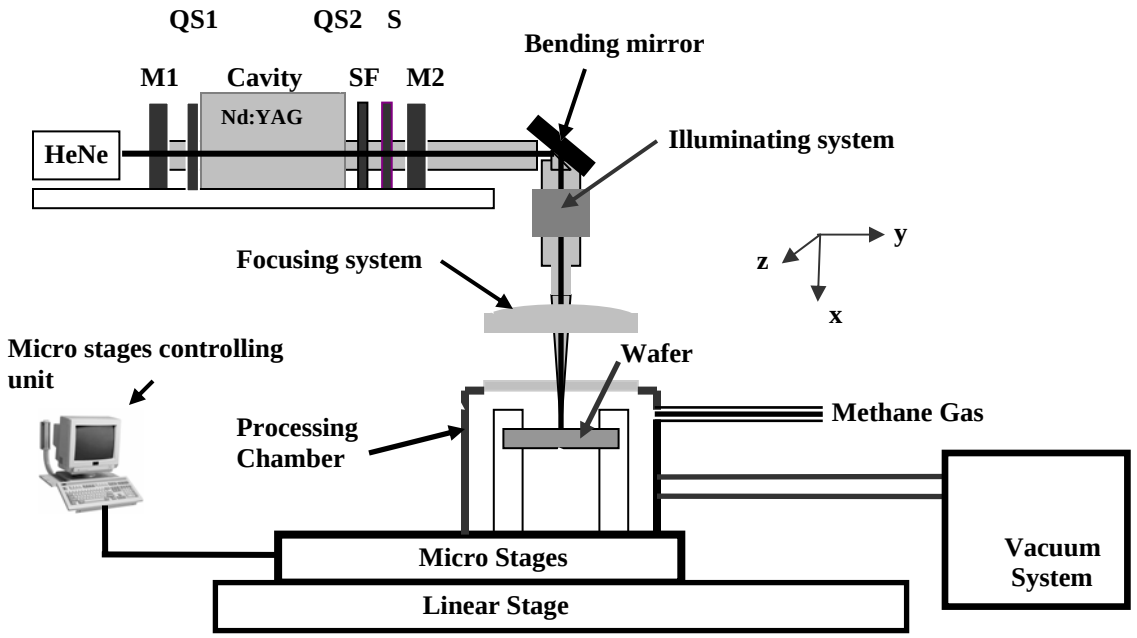


Fig.21: Experimental setup for laser metallization of the SiC chip (Kar Lab).

Laser embedded microstructuring experiments were conducted using a setup shown in Fig. 21. A high intensity Nd:YAG pulsed laser beam (average laser power = 8.5 W, pulse repetition rate = 5 kHz, beam radius at the surface of the sample chip is ~ 55 μm with the laser focal spot being 5 mm above the top surface of the sample chip, laser beam scanning speed = 1 mm/s) was used to create an embedded optical microstructure in SiC chip in the presence of methane gas at 30 psi. This process is known as laser metallization [4-5] in which localized heating by the high intensity laser beam disorders the crystalline structure of SiC chip and produces carbon-rich phases which usually exhibit metal-like properties. The temperature distribution inside the SiC chip sample during laser microstructuring can be expressed as:

$$T(x) - T_a = -\frac{1}{k\eta}(1-R)I_0 . e^{-\eta x} - \frac{(1-R)I_0}{k}x + \frac{I_0 e^{-\eta L}(1-R)(h-k\eta)+(1-R)I_0\eta(k+hL)}{k.h.\eta} \quad (1)$$

for a continuous wave laser beam, where $T(x)$ is the temperature inside the sample at any distance x from the top surface of the sample, $R$ is the reflectivity of the sample at the given wavelength, $k$ is the thermal conductivity of SiC, $h$ is the heat transfer coefficient, $\eta$ is the absorption coefficient of the sample, $L$ is the thickness of the sample, $T_a$ is the temperature of the ambient methane gas and $I_0$ is the irradiance of the Nd:YAG laser.

$T(x)$ was set to the peritectic temperature (2800°C) of SiC in Eq. (1) and the laser irradiance $I_0$ necessary to accomplish microstructuring was estimated and then the required laser power, P, was calculated using the relation $I_0 = \frac{2P}{\pi r_0^2}$, where $r_0$ is the laser beam radius at its waist. Substituting T = 3073 K, $T_a$ = 300 K, R=0.2, $\eta$=1179.9 $m^{-1}$, k=370 W/m · K for 4H-SiC [6], h=10 $W/m^2$· K, L= 399 μm, x = 200 μm into Eq. (1), P was found to be 8.5 W for $r_0$ = 50.5 μm.

A schematic diagram of the microstructured and non-microstructured sections of the SiC chip is presented in Fig. 22, showing the incident and reflected He-Ne beams in both sections. The reflected power from the non-microstructured section of the chip is oscillatory as shown in Fig. 20. In other words, this reflected power does not increase or decrease monotonically with respect to temperature. The oscillatory pattern is produced because the incident He-Ne beam undergoes multiple reflections at the top and bottom surfaces of the chip, generating multiple beams that interact with one another and the incident laser beam, leading to multibeam interference.

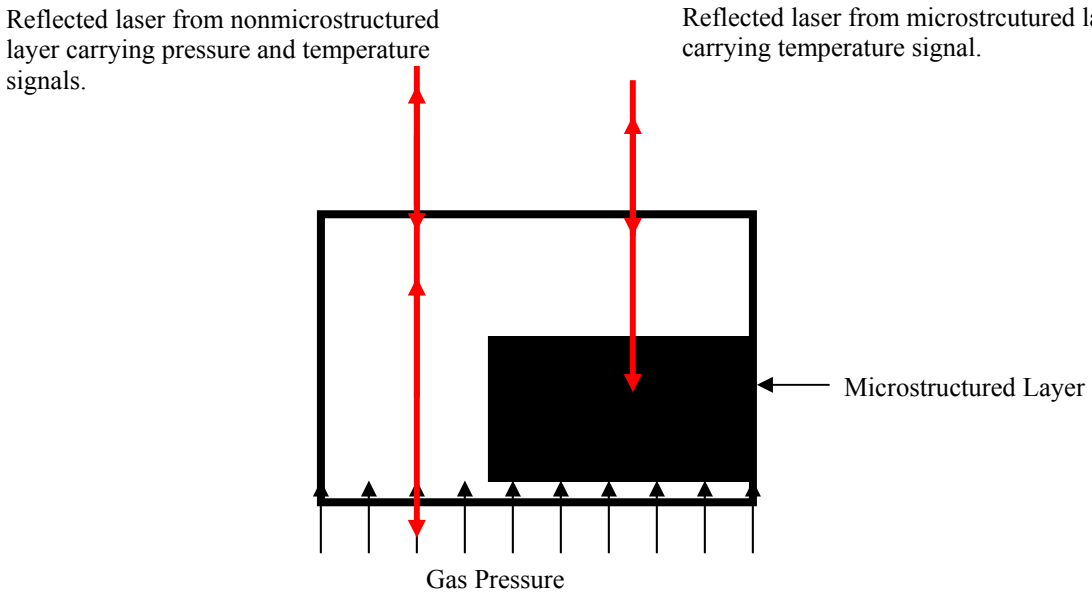


Figure 22: Sensor design with microstructured and non-microstructured sections.

The interference pattern in Fig. 20 is a multivalued function of temperature. A single valued function, however, is useful for a functional sensor. This functionality can be created in the SiC chip by means of the microstructured layer. The optical responses of a laser- microstructured layer are presented as a function of temperature in the temperature ranges of 20-500°C and 20-700°C in Figs. 23 and Fig.24, respectively. The results show that the oscillations of the reflected power are negligibly small compared to the oscillations in Fig. 20. So the reflected power in Figs. 23 and Fig.24 can be considered as a monotonic function of temperature. This characteristic of the microstructured SiC sample (see Fig.25) enables it to be a potential temperature sensor.

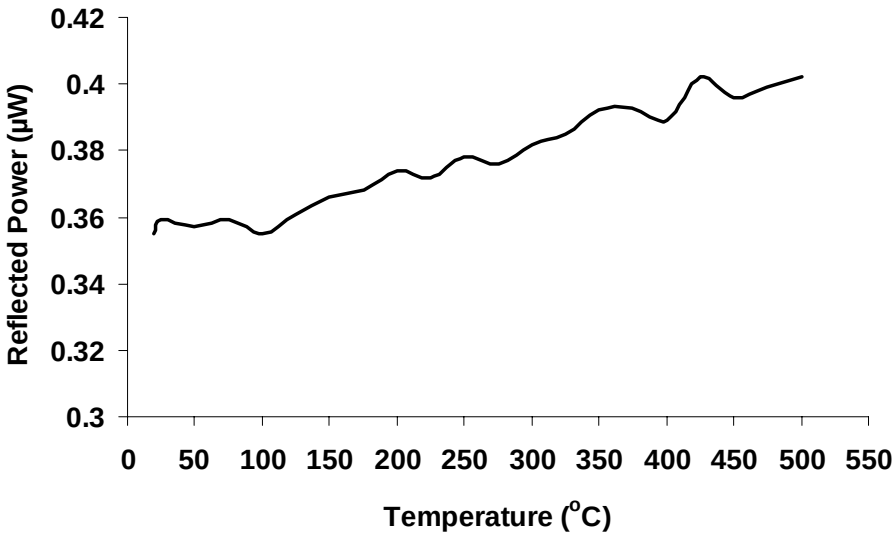


Figure 23. Reflected power from microstructured SiC chip section as a function of temperature up to 500°C at normal incidence angle of the laser beam.

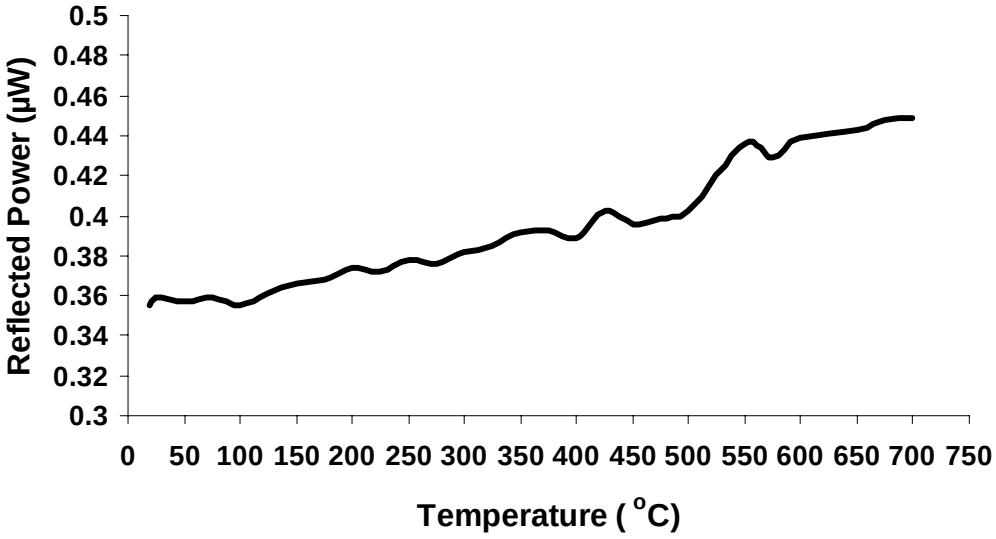


Figure 24. Reflected power from microstructured SiC chip section as a function of temperature up to 700°C at normal incidence angle of the laser beam.

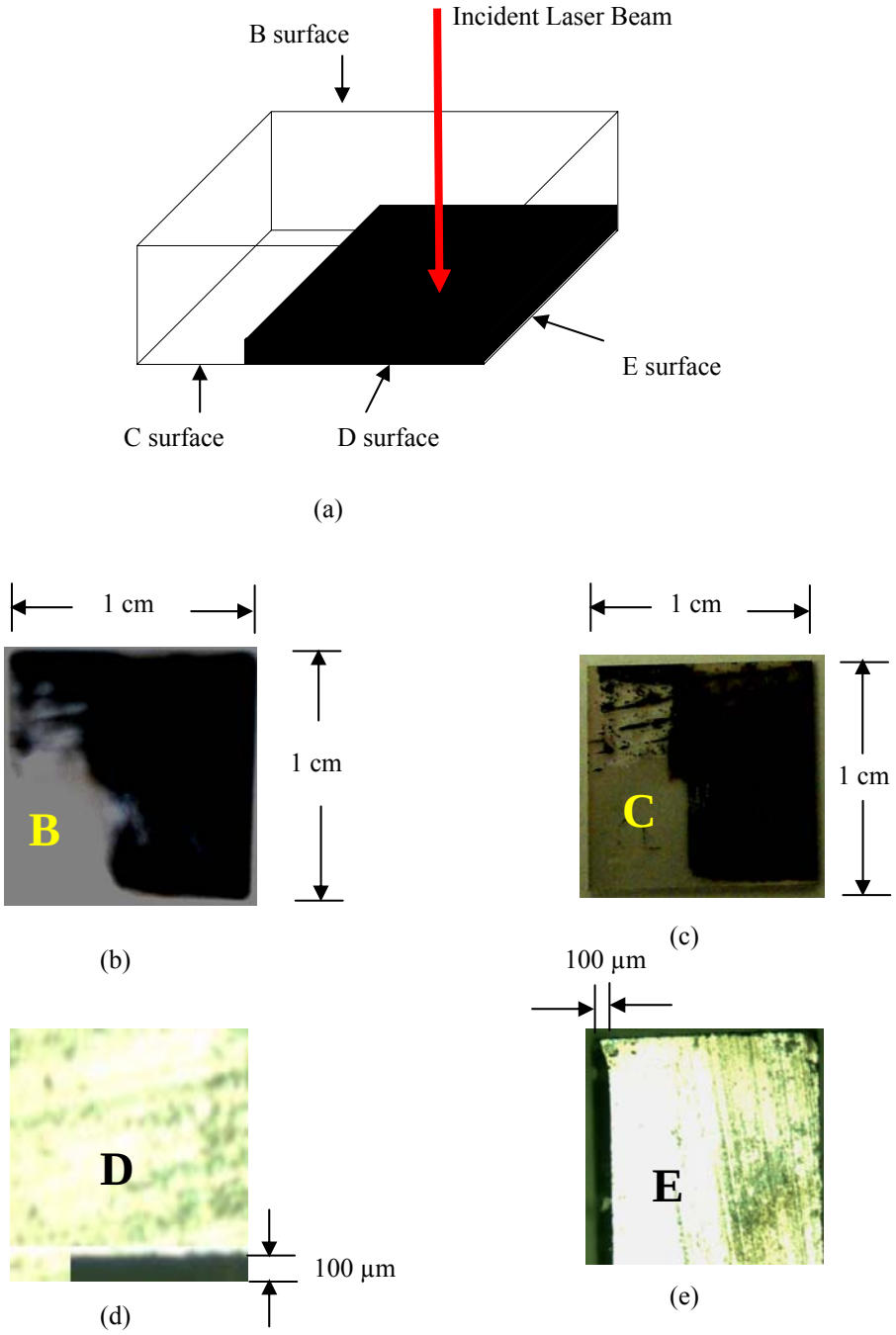


Figure 25. Geometrical sketch and photos of laser-fabricated SiC chip: (a) Schematic drawing of a SiC chip showing the laser-embedded sensing microstructure, (b) View for top surface B showing the top view of the microstructure, (c) View for bottom surface C at which the growth of the chip microstructure nucleated for this sample, (d) View for side surface D showing the thickness of the embedded chip and (e) View for side surface E showing the thickness of the embedded SiC chip.

Applicote Associates (via Kar LAMP LAB UCF) provided the fabricated 6H-SiC parent wafers for embedded optical phase fabrication. These wafers needed to be diced to a square shapes with perfect dimension so that the chip can fit into the Kar LAB experimental setup with maximum gas sealing for experiments at high temperatures and high pressures. However, dicing or sectioning of these wafers using existing diamond saw technologies (e.g., Inrad, Valley Design Corporation) or laser-water jet technologies (Synova) are becoming prohibitively expensive. Within the constraints of this project, developed is a simple approach using a very sharp diamond saw blades as a scribe, scribing 1 cm x 1cm grid in the wafer, placing a scribed corner or edge of the wafer on a rectangular metal substrate aligning the scribe lines with the metal substrate edges, then tapping on the scribe lines. This approach has proved adequate for our limited sample requirements for Kar LAB embedded optical phase microstructured processing.

## H: RESULTS AND DISCUSSION

### Sensor Probe Elements Industrial Feasibility Assessment Study:

First time batch fabrication and assembly of the 6-H SiC chips shows a ~ 25% yield of good chips that can be deployed in the proposed sensor probe. This study is conducted using analysis of chip visible light interferograms where a low fringe count chip is considered better for probe design.

A bench-top IR probe design is implemented to test sensor performance based on various industrial power plant conditions such as changes in light polarization, presence of various soot levels on the sensor SiC chip, exposure of the chip to extreme temperature and corrosive chemical environments.

Specifically, a first polarization test is conducted using many linearly polarized beams with the angle of linear polarization sweeping over a $180^o$ range. This is done by using a manually rotated linear polarizer P with a rotation maximum of $90^o$. To produce $90^o$ to $180^o$ polarization rotation, a twisted Nematic Liquid Crystal (NLC-R) cell is electrically turned on so input light polarization is no longer rotated by $90^o$. With the NLC-R on, the manual polarizer P is again rotated through $90^o$. Thus, using NLC-R and manual polarizer P rotation, the SiC chip is exposed to linearly polarized light with different direction of linear polarization in the plane normal to the chip optic axis. Indeed, the interference images do not change in fringe positions as the incident linear polarization is changed. In all cases, the same fringe pattern is maintained; only the image average power changes because of the change in the incident average power due to the manual rotation of P. Next, a polarization test is conducted using many elliptical polarization states using a birefringent-mode parallel-rub phase NLC-P cell that acts as an optical phase shifter for the input vertically polarized light. By controlling the angle of the linear polarizer P and the NLC-P produced phase shift, a variety of elliptically polarized states are generated to test the optical interferometric response of the SiC chip. These interferograms indeed show no fringe pattern change as the input light state of polarization is changed through various elliptical states defined by the classic ellipse eccentricity and tilt parameters. Thus the desired polarization independent operation results show the proposed SiC-based sensors to have a robust sensor design as needed for harsh environment operations where polarizations can vary.

Probe sensor operations are tested using SiC chips exposed to a variety of light, moderate, heavy, and heavy & heat soaked soot conditions on the external face of the chip. Heavy soot shows a clear black external deposit, yet all soot conditions are shown not to effect sensor operations as strong interferograms are measured. Similarly, long heat and acidic chemical soaks do not effect chip interferogram making capability necessary for sensor operations. Vibration within a probe used in an industrial setting can possibly effect sensor operations. Proposed is a probe design to compensate for this vibration using piezo-mechanics for the fiber lens. Initial piezo-mechanics and controls is shown and under testing.

Overall, these initial studies attest to the promise and strengths of SiC chip-based optical wireless sensor technology for fossil fuel based power generation system applications.

**Embedded Optical Phase SiC Chip fabrication and testing for high temperature gas species sensing:**

The Kar LAMP Lab.-UCF has completed a laser system and related temperature and gas feeding mechanics and thermal controls to enable the fabrication of the desired gas species specific optical embedded phase (or microstructures) within a test SiC chip sample. This optical embedded phase (also called laser- microstructured) SiC chip exhibits a monotonic change in the reflected power as a function of temperature, which indicates that it can sense temperature only. Data have been collected from non-microstructured section of the chip that contain the effects of both the temperature and pressure. These data and the response of the microstructured section of the chip need to be analyzed to separate the effects of the pressure from that of the temperature in order to design a pressure-based gas species sensor. Gas species sensing data obtained by using these two section chips will be included in the next report.

AppliCote Associates (AA), LLC (sub. via UCF) has worked with a materials characterization laboratory to modify their sample stage, increasing its sample capacity, of a scanning electron microscope coupled with energy dispersive spectra chemical analysis (SEM/EDS). This approach was taken to economize materials characterization analysis and to allow "same time" evaluation of a group of samples to better understand inconsistencies and trends in processing. As mentioned earlier, the first group of samples scheduled for SEM/EDS analysis is termed "laser-embedded microstructuring" of SiC. Upon completion of the optical response studies of this laser-embedded microstructured optical chip by LAMP Kar Lab., AA will receive the sample from UCF and carry out SEM/EDS studies of the laser-created microstructure that acts as an optical absorber giving rise to its unique characteristics. In the mean time, LAMP Kar Lab. will conduct laser doping of SiC to carry out gas species sensing experiments. Upon completion

of these experiments, AA will receive samples from LAMP Lab. to conduct SEM/EDS studies on laser-doped samples. Depending on the initial results, a few cycles of these iterations may have to be completed to gain insight into the chip performance and optimize the gas sensor response. These cyclic activities are illustrated in Fig. 26.

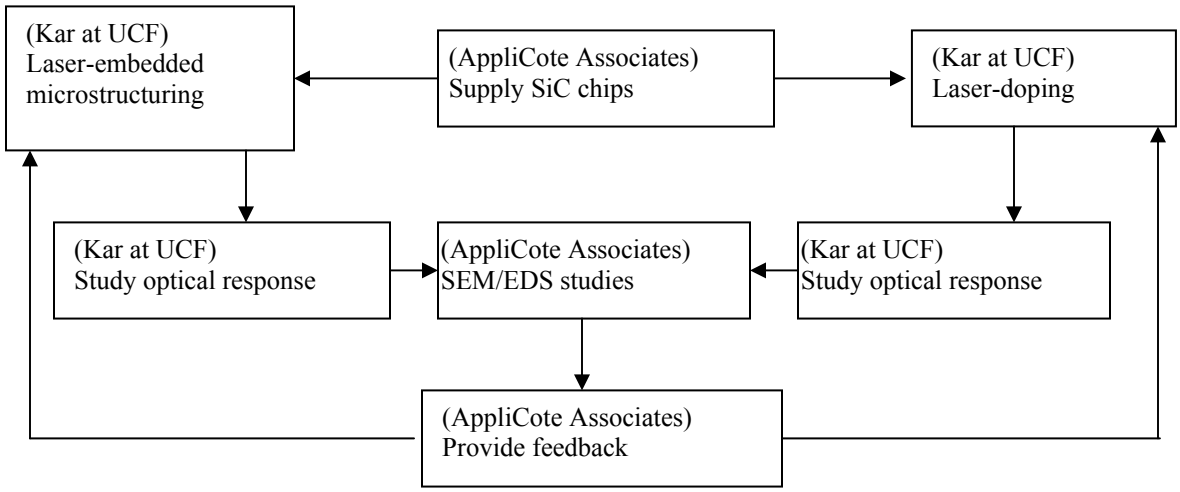


Figure 26. Project activities for SiC chip development, sensor fabrication and optical response studies.

## I: CONCLUSION

In conclusion, this report describes work that has evolved to meet the 2006 April 1 to Sept.30, 2006 Quarter (3 months) stated objectives of (a) conduct a probe elements industrial environment feasibility study and (b) fabricate embedded optical phase microstructured SiC chips for individual gas species sensing. Next, we will focus on meeting objectives of (a) probe design assembly and testing and (b) fabrication and materials characterization of specific embedded phase microstructured SiC chips and testing these chips for individual gas species discrimination.

## J: REFERENCES

[1] R. Duncan, D. Gifford, V. Rajendran, " OFDR tracks temperatures on power generators," Laser Focus World Magazine, p.89, Oct. 2003.

[2] A. D. Kersey, et.al., " Fiber Grating Sensors," IEEE/OSA J. Lightwave Tech., Vol.15, No.8, pp.1442-1463, August 1997.

[3] Brian Culshaw, " Optical Fiber Sensor Technologies: Opportunities and Perhaps Pitfalls," IEEE/OSA Journal of Lightwave Technology, Vol. 22 , No. 1, pp 39 – 50, Jan. 2004.

[4] D. K. Sengupta, N. R. Quick, and A. Kar, Laser Conversion of Electrical Properties for Silicon Carbide Device Applications, *Journal of Laser Applications*, vol. 13, 2001, pp. 26-31.

[5] I. A. Salama, N. R. Quick, and A. Kar, "Laser Direct Writing and Doping of Diamond-like Carbon, Polycrystalline Diamond and Single Crystal Silicon Carbide," *Journal of Laser Applications*, Vol. 16, 2004, pp. 92-99.

[6] Goldberg Yu., Levinshtein M.E., Rumyantsev S.L. *Properties of Advanced SemiconductorMaterials GaN, AlN, SiC, BN, SiC, SiGe* . Eds. Levinshtein M.E., Rumyantsev S.L., Shur M.S., (John Wiley & Sons, Inc., New York, 2001), pp. 93-148.